CNT-PVDF Composite Flow-Through Electrode for Single-Pass Sequential Reduction-Oxidation

Supporting Information

Journal of Materials Chemistry A

Revised December 18th 2013

Guandao Gao,[1,2] Qiaoying Zhang,[1] Chad D. Vecitis[1*]

School of Engineering and Applied Sciences, Harvard University, Cambridge, MA 02138[1]

Key Laboratory of Pollution Processes and Environmental Criteria (Ministry of Education), College of Environmental Science and Engineering, Nankai University, Tianjin 300071, China[2]

[*] *Corresponding author: Chad D. Vecitis,*
Email: vecitis@seas.harvard.edu, Phone: (617) 496-1458.
Address: School of Engineering and Applied Sciences, Harvard University,
Cambridge, MA 02138

Phase Inversion

The casting solution was placed in an ultrasonic bath (Branson 2100) for 60 min to remove any bubbles and dissolved gas then left to stand overnight in the dark. The casting solutions were spread onto a glass plate using an automatic film applicator (Elcometer 4340 Automatic Film Applicator) using a bar coater (Elcometer) of 100-μm thickness. Immediately after spreading, the glass plate with casting solution film was immersed in a pure water non-solvent coagulation bath for phase inversion. After the CNT-PVDF separated from glass plate, the film was placed in a DI water bath at 30 ^{o}C for 24 h to remove any residual solvent.

Electrochemical Impedance and OCPT Experiments

Electrochemical impedance spectroscopy (EIS) was completed at a potential amplitude of 5 mV scanned over a frequency range of 0.1 to 10^5 Hz at different oxidation or reduction potentials. The resultant data were simulated with Nyquist and Bode plots. The total cell voltage (0 - 4.0 V) distribution between cathode and anode were recorded by measuring the open circuit potential vs. time (OCPT) for each electrode in separate experiments.

Calculation of Molar Carbon Balance

The carbon balance during the steady-state flow-through electrochemical experiments was calculated using the influent NB as determined by TOC & UPLC-UV analysis and the effluent NB, NSB, and An as determined by UPLC-UV analysis and the effluent bicarbonate/carbonate by TIC analysis. The TOC/TIC mgC L^{-1} values were converted to molarity carbon by the equation: $[C] = (gC\ L^{-1}) \times (0.083\ moleC\ gC^{-1})$ assuming 1 C per molecule. The UPLC-UV values were converted to moleC by assuming 6 C per NB/NSB/An molecule. The % carbon balance for each individual molecule was calculated by taking the effluent moleC for that molecule and dividing by the influent moleC for NB. Unaccounted carbon was labeled unknown. The UPLC-UV, TOC, & TIC calibration and analysis are described in the text.

Ease of An vs. NB Electrooxidation: Steady-state and EIS Results & Discussion

Over a steady-state CNT anode potential range of +0.9 to +2.1 V, the effluent aniline concentration is observed to decrease linearly with increasing potential. In contrast, CNT anode potentials up to +2.1 V have negligible effect on effluent NB concentrations. The effluent NB is observed to decrease slightly at 0 V due to the strong, rapid sorption of NB to the CNTs, 25-35 mg g-1,[1] via interaction of the positive, electron withdrawing nitro-group with the electron-donating CNT π-bonds. The effluent NB then increases at the first applied anode potential (+0.9

V) due to electrostatic desorption, as previously observed for positively-charged methylene blue.[2] In regards to the EIS, the measured charge transfer resistance (R_{CT}) is 153 ohm at +0.8 V, nearly an order of magnitude greater than 17 ohm observed at the opposite polarity potential, -0.8 V. RCT is inversely proportional to the electron transfer rate ($R_{CT} \sim k_{CT}^{-1}$), confirming the ease of NB reduction vs. oxidation.

Mechanism of NB Reduction-Oxidation

The mechanism of NB reduction-oxidation was examined by wider-range CV (-1.2 to +1.2 V; blue) using two CNT electrodes (Fig. S2E). Six redox peaks are observed and the peak locations are in agreement with previous studies on NB reduction and An oxidation (Table S3).[3-8] In particular, there is good peak location agreement with a study that utilized a CNT cathode for NB reduction.[7] A representative overall reaction scheme is detailed in Fig. S2D with species analyzed in red and redox reactions in blue. Reaction A is the 4-electron reduction of NB to phenylhydroxylamine (PHA). Attempts were made to analyze for PHA, but it oxidized quickly in the ambient atmosphere to nitrosobenzene (NSB). Reactions C1 and C2 represent the reversible 2-electron PHA ↔ NSB redox pair. Reaction B represents the reduction of NB/PHA/NSB to An. Reactions D and E are An oxidation reactions as confirmed by shorter-range cyclic voltammetry (-0.6 to +1.2 V; red) that did not include reaction B (-0.8 V; NB reduction to An) resulting in loss of oxidative peaks and current. Positive working potential CV of pure An (Fig. S2E) displayed peaks D & E as well. However, the oxidation reactions occurring at D and E are likely not degrading An, but rather polymerization since the anode potentials are <1.4 V[7, 8]similar to results for phenol electropolymerization.[9] Initial aniline oxidation products include hydroxylated aromatic and small acid intermediates such as benzoquinone and maleate.[5, 6]

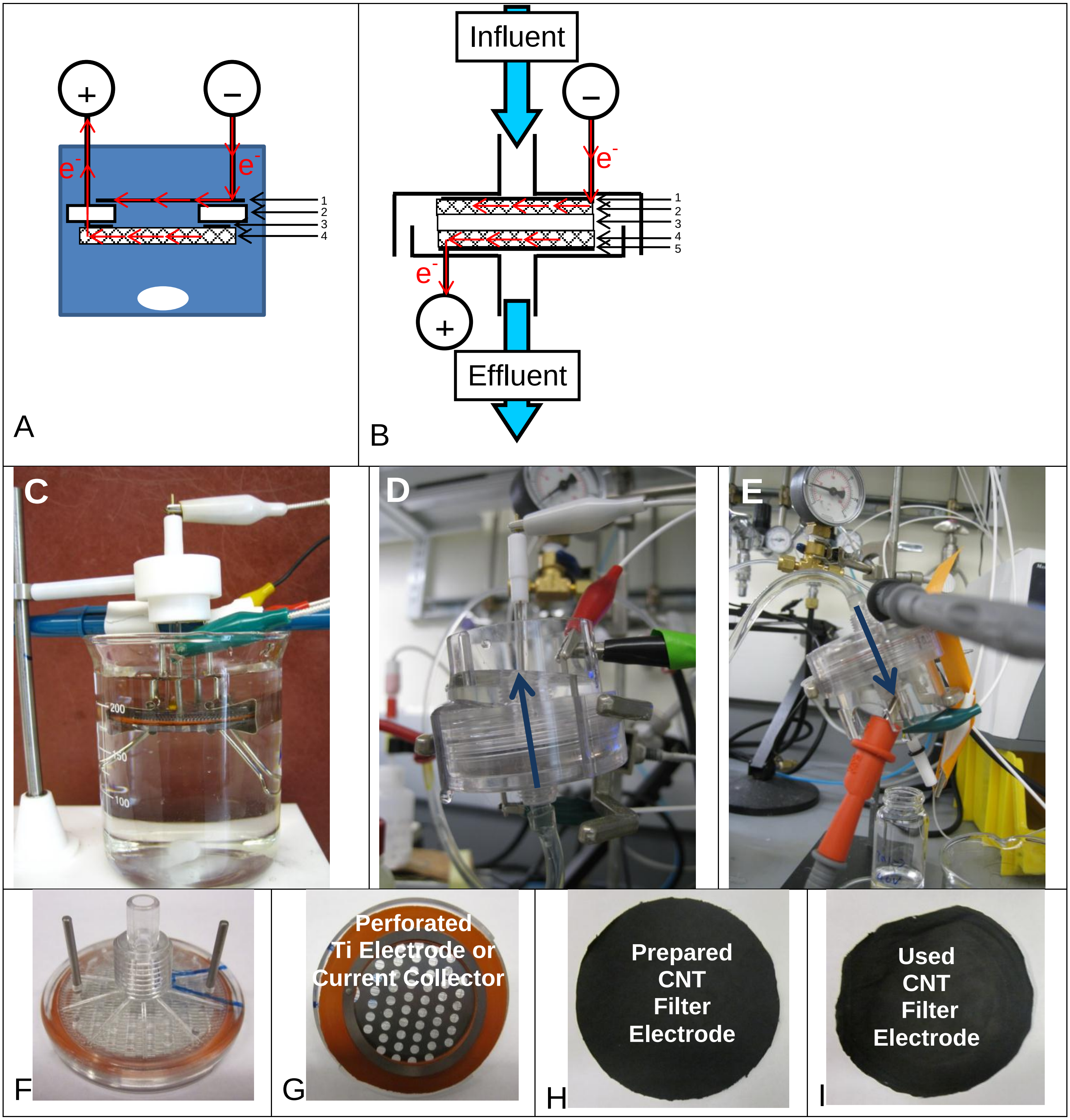

Figure S1. Electrochemical configurations. A) A batch (no-flow) system was used for controlled single electrode characterization e.g., cyclic voltammetry, since most electrochemistry theory assumes presence of a diffusion boundary layer that yields more consistent results where 1) a perforated Ti electrode unless otherwise noted, 2) an insulating silicone rubber electrode separator and seal, 3) if needed, a perforated titanium current collector that is pressed into the carbon nanotube network electrode, and 4) a CNT electrode supported by a PTFE membrane unless otherwise noted. **B)** The flow-through configuration that was used to examine sequential electrochemical redox processes and the effects of internal electrode convection where 1) the CNT-PVDF and perforated Ti current collector, 2) porous CNT electrode, 3) insulating porous PVDF separator, 4) porous CNT electrode, and 5) CNT-PVDF and perforated Ti current collector. **C)** image of batch set-up used for cyclic voltammetry and EIS where clips are red for the counter electrode, green for the working electrode, and white for the reference electrode. **D)** image of the flow set-up used for cyclic voltammetry and EIS where clips are red for the counter electrode, green for the working electrode, and white for the reference electrode. **E)** image of the flow set-up used for the steady-state and OCPT experiments where clips are black for the cathode, red for the anode, green for the working electrode, and white for the reference electrode. **F, G)** Images of the modified filtration casing and perforated Ti electrode. **H, I)** Images of the CNT network before and after low potential electrochemical filtration, respectively.

Figure S2. Electrochemical Characterization of Nitrobenzene and Aniline. Solution conditions were $[NB\text{ or }AN]_{in}$ = 100 μM, $[Na_2SO_4]$ = 10 mM. The cyclic voltammetry were completed at a scan rate of 100 mV s^{-1} and the electrochemical impedance spectrums were completed using potential amplitude of 5 mV over a frequency range of 0.1 to 10^6 Hz at varying work potential. **A)** Positive working potential CV from 0 to +1.5 V of nitrobenzene using various working electrode materials and a perforated Ti counter electrode at J = 0 mL min^{-1}, **B)** Steady-state oxidation of 100 μM NB (black) and An (red) at anode potentials of 0 to 2.1 V at J = 1.6 mL min^{-1} where the solution first flows through a Ti cathode and then a CNT anode, **C)** Nyquist plot of nitrobenzene EIS at various work potentials using a CNT working electrode and a Ti counter electrode at J = 0 mL min^{-1}, **D)** plausible reaction mechanism with steps labelled to match CV peaks from E and species quantified here in red, **E)** CV starting at 0.0 V from 1.2 V to -1.2 V (blue) or -0.6 (red) at 100 mV s-1 with J = 0 mL min-1 using a Ti counter and CNT working electrode, and **F)** potential distribution by OCPT between cathode (dashed) and anode (solid) as a function of relative CNT filter masses of 1.5:1 (red), 1:1 (blue), and 1:1.5 (black) at different applied voltages determined by individual open circuit versus potential experiments where the solution flows through the CNT cathode then the CNT anode at J = 1.6 mL min^{-1}.

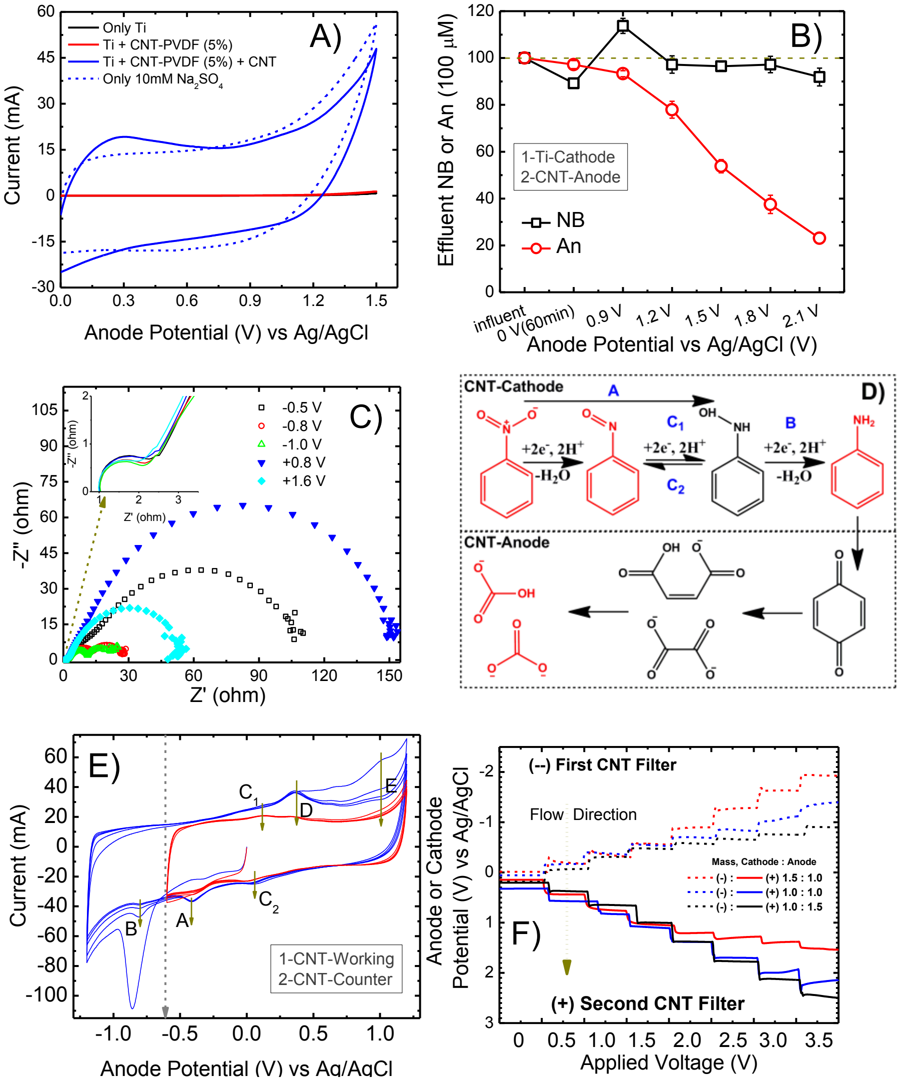

Table S1. Properties of the Electrochemical Filter Materials.

Material	Contact Angle (°)	Bulk Porosity (%)	Thickness (μm)	Permeability (LMH/bar)	Resistance (Ω)	Mechanical Properties		
						Ultimate Strain (%)	Strength (Pa)	Young's Modulus (Pa)
Ti	N/A	N/A	N/A	N/A	<1.0	N/A	N/A	N/A
PVDF	79.1±3.2	80.3±4.9	47.3±0.5	>6000	$>2\times10^{6}$	0.137±0.032	$7.91\pm0.22\times10^{5}$	$1.91\pm0.45\times10^{7}$
CNT	100±2.1	86.1±2.4	51.3±3.7	510±20	<1.0	0.020±0.003	$3.83\pm0.13\times10^{6}$	$2.77\pm0.26\times10^{8}$
1%-CNT-PVDF	73.0±2.0	92.4±4.4	46.7±1.7	>6000	$>2\times10^{6}$	0.166±0.041	$8.93\pm0.86\times10^{5}$	$2.43\pm0.22\times10^{7}$
3%-CNT-PVDF	70.7±2.5	82.8±5.7	51.3±3.7	>6000	210±27	0.170±0.041	$9.11\pm0.77\times10^{5}$	$3.09\pm0.45\times10^{7}$
5%-CNT-PVDF	66.2±3.9	81.0±11.3	48.2±1.9	>6000	60±12	0.100±0.034	$1.06\pm0.15\times10^{6}$	$5.26\pm0.70\times10^{7}$
5%-5-Layer	66.2±4.1	81.4±12.4	211.7±3.3	180±30	5.3±1.2	N/A	N/A	N/A

Table S2. Electrochemical parameters from the simulated EIS spectra.

	Potential	R_{ct}	W_{mt}
Oxidation	+ 0.8 V	153.1	N/A
	+ 1.6 V	61.2	N/A
Reduction	- 0.5 V	112.5	N/A
	- 0.8 V	16.6	8.7
	- 1.0 V	12.2	13.1

Table S3. Previously reported NB/NSB/An redox potentials.

Reaction A (nitrobenzene to phenylhydroxylamine)						
Reference	***Solvent***	***Cathode***	***pH***	***E***	***Reference***	***Method***
[4]	Water	Dropping Mercury	5.7 7.4 9.2	-0.48 -0.58 -0.70		LSV
[10]	Water	Glassy Carbon	6.0 7.0 8.0	-0.72 -0.72 -0.68	Ag/AgCl	CV
[3]	Water-MeOH 93:7	Devarda Cu Raney Ni	7.1 0.14 M NaOH	-0.6 -1.0	SCE	Batch (Aniline product)
[11]	Water	CNT (graphite)	5.0	-0.6	SCE	CV
[12]	Water-Micelles	Mercury Drop	7.1	-0.7 to -0.85	SCE	CV
This Study	Water	CNT	neutral	-0.4	Ag/AgCl	CV
Reaction B (phenylhydroxylamine to aniline)						
[10]	Water	Glassy Carbon	9.0	-0.8	Ag/AgCl	CV
[3]	Water-MeOH 93:7	Devarda Cu Raney Ni	7.1 0.14 M NaOH	-0.6 -1.0	SCE	Batch (Aniline product)
[11]	Water	CNT (graphite)	5.0	-0.85	SCE	CV
This Study	Water	CNT	neutral	-0.8	Ag/AgCl	CV
Reaction C1 (nitrosobenzene to phenylhydroxylamine)						
[10]	Water	Glassy Carbon	9.0	-0.4	Ag/AgCl	CV
[11]	Water	CNT (graphite)	5.0	0.1	SCE	CV
[12]	Water-Micelles	Mercury Drop	7.1	0.0 to -0.4	SCE	CV
This Study	Water	CNT	neutral	0.12	Ag/AgCl	CV
Reaction C2 (phenylhydroxylamine to nitrosobenzene)						
[10]	Water	Glassy Carbon	9.0	-0.1	Ag/AgCl	CV
[11]	Water	CNT (graphite)	5.0	0.0	SCE	CV
[12]	Water-Micelles	Mercury Drop	7.1	0.1 to -0.3	SCE	CV
This Study	Water	CNT	neutral	0.05	Ag/AgCl	CV

Reaction D & E (aniline oxidation)						
[6]	Water	PbO_2 Packed Flow Bed (1mm spheres)	2.0	n/a – I = 1,2,3 A		Batch I1) BQ I2)Maleic I3)CO2
[13]	Water	electro-Fenton	3.0	n/a		BQ, HQ, phenol, benzenetriol, fumaric, maleic
[7]	Water	SnO_2-Sb_2O_3-PtO	11.0	2.3 V HOdot		dianiline, HO addition
[8]	Water	BDD	8.7 12.0	1.8 V 1.6 V	SCE	CV <1.4 V polyaniline >3.0 V mineralize
This Study	Water	CNT	neutral	CV 0.4/1.0 V Batch 2.0 V	Ag/AgCl	2.5 V to mineralize

Figure S3. Steady-state current vs. potential (A, B) and characteristic UPLC-UV chromatograms (C-F). A & B are corresponding data for experiments presented in Figure 4E & F, respectively. C-F are steady-state effluent UPLC-UV chromatograms for data presented in Fig. 4B.

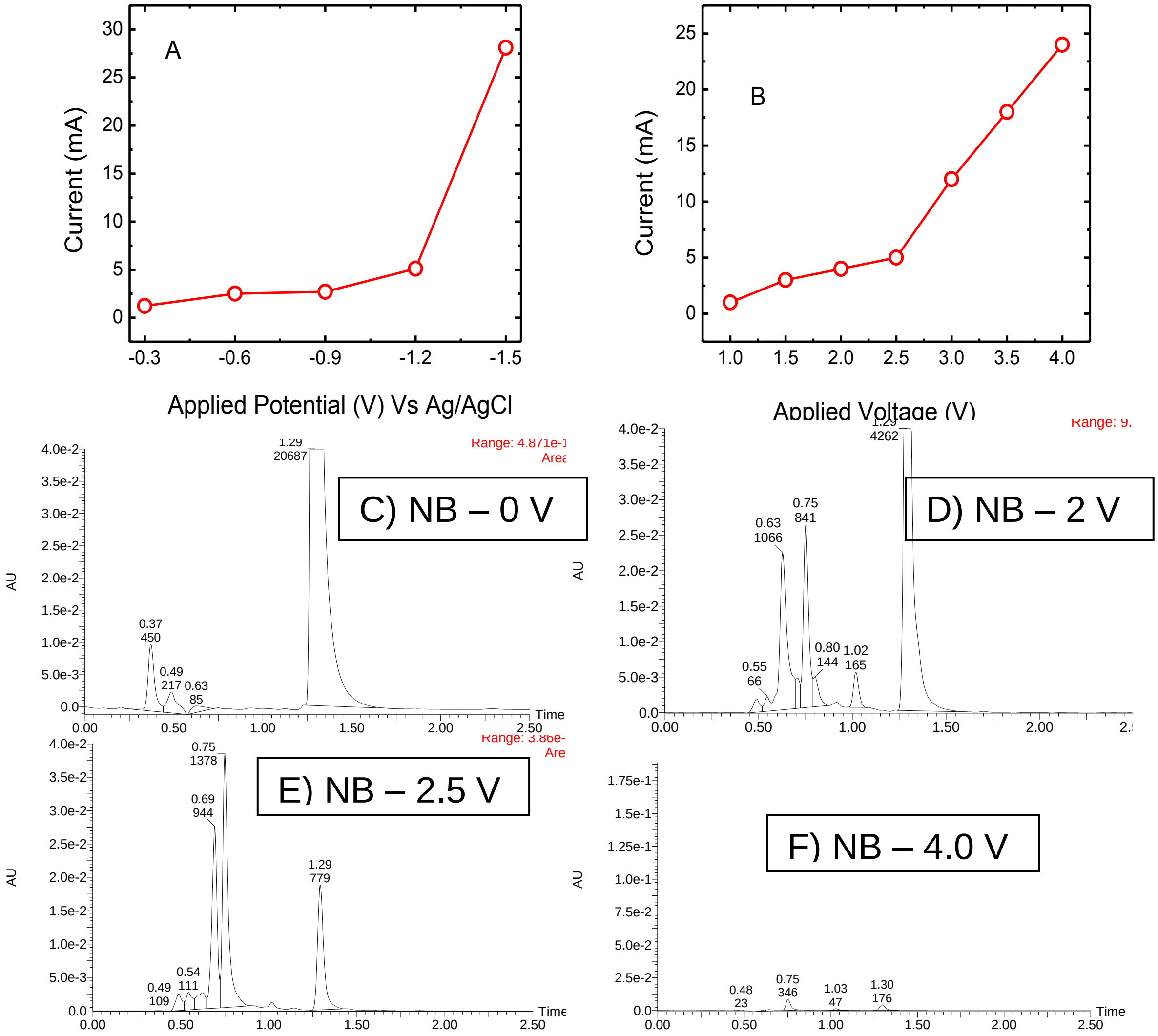

References

1. X.-E. Shen, X.-Q. Shan, D.-M. Dong, X.-Y. Hua and G. Owens, *Journal of Colloid and Interface Science*, 2009, **330**, 1-8.

2. C. D. Vecitis, G. D. Gao and H. Liu, *J. Phys. Chem. C*, 2011, **115**, 3621-3629.

3. A. Cyr, P. Huot, G. Belot and J. Lessard, *Electrochimica Acta*, 1990, **35**, 147-152.

4. J. Pearson, *Transactions of the Faraday Society*, 1948, **44**, 683-697.

5. E. Brillas, E. Mur, R. Sauleda, L. Sanchez, J. Peral, X. Domenech and J. Casado, *Applied Catalysis B-Environmental*, 1998, **16**, 31-42.

6. D. W. Kirk, H. Sharifian and F. R. Foulkes, *J. Appl. Electrochem.*, 1985, **15**, 285-292.

7. Y. J. Li, F. Wang, G. D. Zhou and Y. M. Ni, *Chemosphere*, 2003, **53**, 1229-1234.

8. M. Mitadera, N. Spataru and A. Fujishima, *J. Appl. Electrochem.*, 2004, **34**, 249-254.

9. G. D. Gao and C. D. Vecitis, *ACS Appl. Mater. Interfaces*, 2012, **4**, 1478-1489.

10. C. K. Chua and M. Pumera, *Electroanalysis*, 2011, **23**, 2350-2356.

11. Y.-P. Li, H.-B. Cao, C.-M. Liu and Y. Zhang, *Journal of Hazardous Materials*, 2007, **148**, 158-163.

12. G. L. McIntire, D. M. Chiappardi, R. L. Casselberry and H. N. Blount, *Journal of Physical Chemistry*, 1982, **86**, 2632-2640.

13. E. Brillas, R. M. Bastida, E. Llosa and J. Casado, *Journal of the Electrochemical Society*, 1995, **142**, 1733-1741.